Automatic inspection for phase-shift reflection defects in aluminum web production

F. TORRES,[1] L. M. JIMÉNEZ,[2] F. A. CANDELAS,[1] J. M. AZORÍN,[2] and R. J. AGULLÓ[1]

[1]*Department of Physics, Systems Engineering and Signal Theory, University of Alicante, Alicante, Spain*
[2]*Department of Science and Technology, Division of System Engineering and Automation, University Miguel Hernández, Elche, Spain*

Industrial inspection problems usually require specific and highly complex solutions that can be implemented at a reasonable cost, what has produced a great research and development effort in the field of computer vision. Among these problems, inspection systems for continuous feed production (named as ''web-inspection''), are those that raise the main challenges for the researchers exceeding the current systems capacity. Manual inspection, that is still being used in many cases, does not allow to reach detection guarantees, accuracy, robustness and a high volume that are required in web-based manufacturing.

Keywords: Automatic inspection, computer vision, web-based manufacturing, aluminum production, phace-shift reflection defects

1. Introduction

Automatic inspection systems are generally very specific and require special architectures which allow to obtain the great quantity of product to analyze with the demanded resolutions (e.g., Newman and Jain, 1995)

The aluminum sheets are obtained with the phase of alloys melting at temperatures between 690°C and 710°C. It is solidified at a temperature between 200°C and 270°C adopting the form of sheet that is bobbin. This sheet is laminated during extrusion process in several stages that permit to obtain different thickness.

Defects detected in the considered system are produced randomly in aluminum sheets during extrusion process when exists an eccentricity disarrangement in the rollers that achieves this process, causing undesirable microscopic vibrations. This causes no homogenous thickness zones at microscopic levels in the aluminum sheets. When this is produced, the faces of aluminum sheets have certain cross-bands in relation with the advance direction. According to the illumination angle on the faulty zone in the sheet, the bands may be seen. No kind of striped pattern is observed in zones without defects.

The defects nature produced on the product to analyze have caused a careful design of the illumination conditions that permits to segment and to identify in a correct form the microscopic deformation produced in the production process. The analyzed defect does not present a dimensional component at a macroscopic significant level but appears as a variation of the reflection angle of the light waves under a certain angle of incidence. Beléndez (1996) and Casas (1994) reported that this process produces a phenomenon of interference characterized by a periodic alteration in the phase and amplitude of the incident wave. Methods based in texture analysis do not present a correct application because defects are not produced at a macroscopic

(a) (b) (c)

Fig. 1. Images captured without coherent light: samples (a) correct, (b) wide and (c) narrow.

level in the material texture. The defect presents a great directionality through the roller's axis appearing periodically on the aluminum surface (Brzakovic and Sari-Sarraf, 1994; Morris and Notarangelo, 1994).

The solution is based in the detection of distortion patterns of structured light, when it falls upon the aluminum surface, because of the different reflection angle caused in the material during the productive process.

2. Detection algorithm

The use of coherent light formed by a single wavelength permits disacouple the diffraction phenomenon between different wavelengths. When the laser beam falls upon the aluminum surface on a faulty product, causes a phase-shifting between the reflected waves that are projected on a screen. If a non-coherent light is used, the correct product cannot be distinguished from the faulty one, as it can be noticed in Fig. 1.

The produced phase-shifting in the coherent light causes the interference between the different reflected waves being generated a interference pattern formed by periodic bands (thin skeletons). The distance between these bands depends, according to the ondulatory optics, on the incident wavelength and on the dimension and type of the defect bands on the analyzed surface (Hetch and Zajal, 1974) (Fig. 2b and c).

Due to the alignment of the considered defect, the interference register captured by the camera shows a radial periodicity. As it can be observed, the difference between the three test images is clear. The correct sample is uniform, the interference phenomenon is null, but in samples with vibrations there are horizontal-arch shaped waves. In the narrow vibration sample, there are distribution of the interference pattern is more dense than in the wide vibration one, showing thinner an closer waves (Fig. 2c).

This interferencial information is collected by a CCD sensor and used to make the defect segmentation. This periodical behavior can be analyzed and classified in a robust way through the frequency analysis, more specifically using the power spectrum of the image (Oppenheim and Wilsky, 1996).

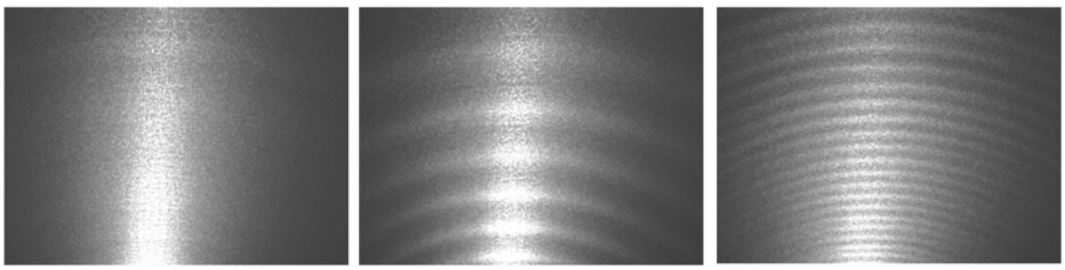

(a) (b) (c)

Fig. 2. Images captured with the structure of Fig. 1: samples (a) correct, (b) wide and (c) narrow.

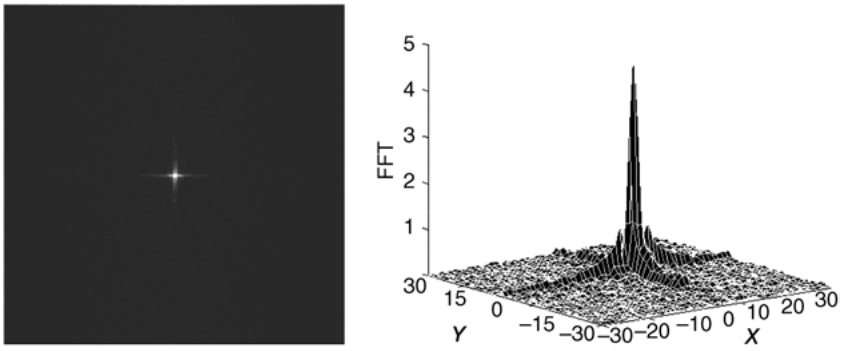

Fig. 3. (a) Fourier spectrum of a correct sample and (b) its 3D representation.

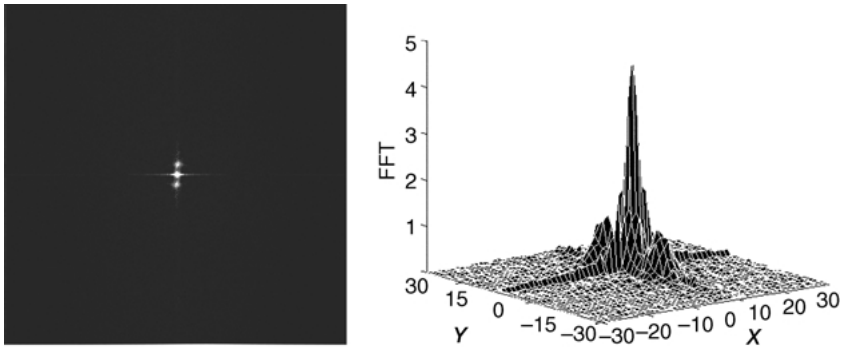

Fig. 4. (a) Fourier spectrum of a sample with wide vibration and (b) its 3D representation.

The interference signal can be modeled as a combination on random distribution functions with a certain displacement that will be translated into an echo in the frequency spectrum. To reduce the computational cost, and based on the finite scope of images, the power spectrum (Fourier transform of the function of autocorrelation of the signal) is approximated by the squared magnitude of the discrete Fourier transform calculated using the FFT algorithm.

Considering that only exists radial displacement, the sampled image can be considered as the combination of echoes displaced *dr*. The periodic term of the interference image will have fundamental frequencies of 1/*dr* (high-frequency signals). The image dependent component will be composed of low-frequencies.

In could be observed the corresponding power spectrum for a correct sample (Fig. 3) and faulty samples with wide (Fig. 4) and narrow vibrations (Fig. 5). The central peak in the spectra corresponds to the term of autocorrelation, and the small two peaks upper and lower stand for the periodic components of the interference. The phase graph does not present a discriminative power that allow to segment the defect.

Taking a look to a transversal significant section of the FFT for each kind of sheets a central point due to the autocorrelation term can always be observed. In the correct sample (Fig. 6), this point is the only meaningful and the rest ones are so small that they are not considered. For faulty sheets, there are another significant points at a d_p distance from the center (Figs 7 and 8). These points correspond to the periodic interference component. This distance will be used later to discern between narrow vibrations from wide ones.

In Section 3, the method to detect incorrect sheets and to distinguish between incorrect sheets with narrow vibration from those with wide vibration will be presented.

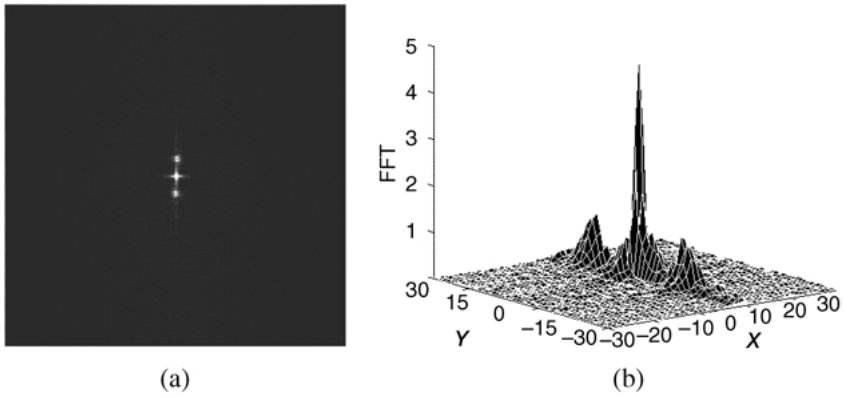

Fig. 5. (a) Fourier spectrum of a sample with narrow vibration and (b) its 3D representation.

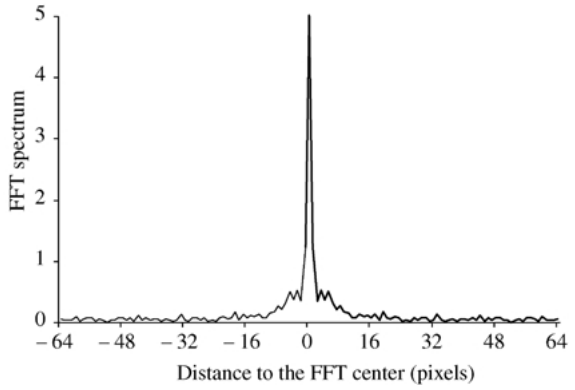

Fig. 6. Transversal significant section of the FFT of a correct sample.

3. Classification algorithm

The first step of detection algorithm consists of calculating 2D FFT in the center of an aluminum sheet image and taking its four most significant peaks. (The central peak corresponding to the image autocorrelation is rejected as its present in all cases.) From each peak, the amplitude that it gets and the distance from the FFT center is calculated.

The selection of the four most significative peeks is carried out looking for the local maxima values of the FFT in both sides around the central peek due to autocorrelation. In order to filter those local maxima produced by noise, a local gradient in both sides of the peak is calculated. Only those local maxima with a gradient higher than a threshold is considered as

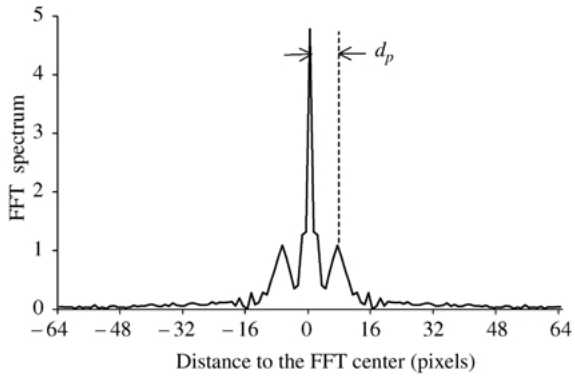

Fig. 7. Transversal significant section of the FFT of a sample with wide.

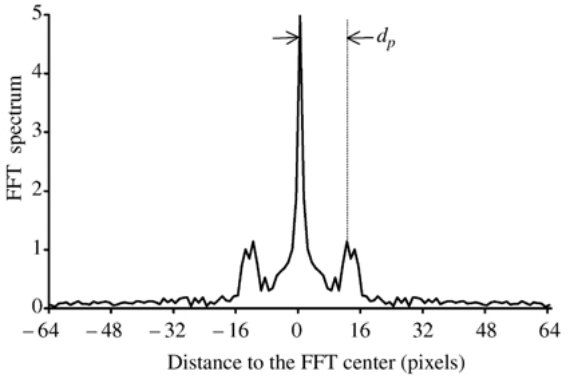

Fig. 8. Transversal significant section of the FFT of a sample with narrow vibration.

Fig. 9. Structure used to detect defects in aluminum sheets.

meaningful peaks. The algorithm selects the firsts two peaks with higher amplitude for each side.

Then, an estimator is generated for each spectrum through the multiplication of the amplitudes by the distance to the center of the FFT for each of the most significant peaks. If the estimator gets a value higher than a sheet inspection threshold, the sample is classified as an incorrect one. In other case, this will be correct. To classify incorrect sheets, the distance of the most significant peaks and a classification threshold are used.

The parameters that are used to classify a sheet are:

- *Inspection threshold*: Maximum value that the calculated characteristic (product of the amplitude by the distance to the center of the FFT of the most significant peaks) can reach to classify a sample as correct one.
- *Classification threshold*: Maximum distance to the FFT center where a peak can be placed to classify a sample as a wide one.
- Amplitude and distance of the four most significant peaks of the 2D FFT from the center of the image.

4. Results

The aim of the first developed prototype (Fig. 9) is to detect defects, although this is not done in real time as it was no required a full product quality control. The achieved precision permits to detect stripes with a thickness till 1 mm, on images captured at a period of 1 s, what means an inspection of 1 m of the sheet each 2.5 m.

Within the scope of the pilot project, the system was tested over a period of several months, on a production line of aluminum. The global results obtained are fully satisfactory, rejecting 1.6% of incorrect sheets and 4.8% of correct sheets, that in many cases are other kinds of defects different to the ones that are to detect. Presently, the system is operative in production line.

In Tables 1–3, the values of the amplitude of the four most significant peaks from the spectrum, as well as its distance and the generated characteristic for five correct samples and 10 incorrect ones (five with narrow vibration and five with wide vibration) are shown.

Table 1. The product of amplitude by distance is always less than the inspection threshold (5)

	Results obtained in correct samples											
	Amplitude of peak no.				*Distance of peak*				*Product of amplitude by distance*			
	A1	A2	A3	A4	D1	D2	D3	D4	A1*D1	A2*D2	A3*D3	A4*D4
1	0.432173	0.316163	0.262270	0.225347	6	10	15	18	2.593038	3.161630	3.934050	4.056246
2	0.450365	0.319351	0.301232	0.228945	5	9	7	12	2.251825	2.874159	2.108624	2.747340
3	0.391940	0.318175	0.263764	0.254018	6	9	11	13	2.351640	2.863575	2.901404	3.302234
4	0.839152	0.454084	0.298171	0.266362	3	6	10	13	2.517456	2.724504	2.981710	3.462706
5	0.659011	0.372998	0.301194	0.215367	4	6	13	10	2.636044	2.237988	3.915522	2.153670

Table 2. For each sample, there is always a peak whose product of amplitude by distance is greater than the inspection threshold (5) and the distance is less than the classification threshold (10)

	Results obtained in samples with wide vibrations											
	Amplitude of peak no.				*Distance of peak*				*Product of amplitude by distance*			
	A1	A2	A3	A4	D1	D2	D3	D4	A1*D1	A2*D2	A3*D3	A4*D4
1	1.068420	0.986409	0.831802	0.607617	3	6	9	11	3.205260	5.918454	7.486218	6.683787
2	0.954612	0.931044	0.625547	0.393771	3	6	8	11	2.863836	5.586264	5.004376	4.331481
3	0.903634	0.641262	0.408357	0.302113	7	9	12	16	6.325438	5.771358	4.900284	4.833808
4	0.949567	0.749569	0.357629	0.331056	7	9	14	16	6.646960	6.746121	5.006806	5.296896
5	1.217390	0.839944	0.452237	0.260372	2	7	10	15	2.434780	5.879608	4.522370	3.905580

Table 3. For each sample, there is always a peak whose product of amplitude by distance is greater than the inspection threshold (5) and the distance is larger than the classification threshold (10)

	Results obtained in samples with narrow vibrations											
	Amplitude of peak no.				*Distance of peak*				*Product of amplitude by distance*			
	A1	A2	A3	A4	D1	D2	D3	D4	A1*D1	A2*D2	A3*D3	A4*D4
1	1.089420	0.711124	0.643861	0.376279	13	5	16	21	14.16264	3.555620	10.30177	7.901859
2	1.088510	0.912718	0.873550	0.630106	3	12	14	7	3.265530	10.95261	12.22970	4.410742
3	0.657449	0.639575	0.454521	0.398082	4	13	6	15	2.629796	8.314475	2.727126	5.971230
4	0.797960	0.708909	0.626024	0.197760	13	5	10	25	10.37348	3.544545	6.260240	4.94400
5	1.049050	0.563855	0.334288	0.323094	13	4	20	9	13.63765	2.255420	6.685760	2.907846

At the present time, a second prototype is being developed that will permit to make the inspection of all whole sheet in real time.

References

Beléndez, A. (1996) *Fundamentos de Óptica para Ingeniería Informática*, University of Alicante Press, Alicante, Spain.

Brzakovic, D. and Sari-Sarraf, H. (1994) Automated inspection of nonwoven web materials: a case study. *Proc. SPIE*, **2183**, 214–223.

Casas, J. (1994) *Optics*, Librería General Zaragoza, Zaragoza, Spain.

Hetch, E. and Zajac, A. (1974) *Optics*, Addison-Wesley.

Morris, J. and Notarangelo, J. (1994) Machine vision metal inspection. *Proc. SPIE*, **2183**, 130–136.

Newman, T. S. and Jain, A. K. (1995) A survey of automated visual inspection. *Computer Vision and Image Understanding* **61**(2).

Oppenheim, A. V. and Wilsky, A. S. (1996) *Digital Signal Processing*, Prentice Hall.